



**Western Region Technical Attachment
No. 94-28
September 6, 1994**

A SPLITTING STORM IN SOUTHWEST IDAHO

David B. Billingsley - WSFO Boise, ID

Introduction

Results from three-dimensional numerical cloud model simulations suggest a strong relationship between environmental vertical wind shear and buoyancy, and the structure and evolution of thunderstorms (Weisman and Klemp 1982, 1984). A balance between these two environmental parameters is apparently necessary to support certain long-lived modes of convection such as supercells and severe multi-cellular storms.

For instance, given enough instability for convection, a moderate-to-strong unidirectional shear profile should produce an updraft that splits into two individual storms which move to the left and right of the environmental wind, respectively (Fig. 1a,b). Rotation associated with the left-moving updraft is shown to be in the anticyclonic sense while the right-moving updraft rotates in the more familiar cyclonic direction (Klemp and Wilhelmson 1978a,b; Wilhelmson and Klemp 1978; Klemp 1987).

In this attachment, an observational example of a splitting storm on 27 May 1994 in southwestern Idaho is compared to these theoretical concepts of storm structure and evolution.

Synoptic Setting

On the morning of 27 May 1994, a 500 mb trough was located on the Washington-Oregon coastline, placing Idaho in a southwesterly upper flow pattern (Fig. 2). A segment of the jet stream was positioned in southeast British Columbia-Western Alberta, trailing back into eastern Washington and Oregon. This location placed southwest Idaho in an area of favorable ageostrophic divergence as shown in Moore and VanKnowe (1992), and contributed to the increased vertical wind shear. At the surface, a cold front was situated from central Montana to southcentral Idaho, with a weaker stationary segment extending west-southwestward into the northern Nevada-California area (not shown).

Quasi-geostrophic diagnostics (using the NGM PC-GRIDDs dataset at 1200 UTC) depicted an area of layer-averaged Q-vector convergence in the mid-troposphere (700-400 mb average) over southwestern Idaho-eastern Oregon-northern Nevada at 1800 UTC (Fig. 3). Examination of layer-averaged Q-vector convergence centered at other levels revealed a similar pattern. Model produced lifted indices were in the 0 to -1 range across this same area (Fig. 4). This combination of QG forcing and instability is supportive of synoptic-scale upward motion across the region of concern. It is interesting to note that the model-derived, net vertical motion was DOWNWARD (though weak at @ 1.5 ubars/sec) in the mid-troposphere, implying that factors other than QG-type forcing in the model were probably more dominant (i.e., diabatic heating, radiation, model terrain effects, etc.).

As indicated, several features appeared to confirm that synoptic-scale ascent and destabilization were taking place over southwest Idaho, prior to and near the time of convective initiation. These included a favorable position of a cyclonically curved jet stream, a nearby surface front, an upstream mid-tropospheric trough, and a moderate amount of static instability.

Sounding Analysis

The 1200 UTC 27 May 1994 Boise sounding was modified for the afternoon hours using a combination of PC-GRIDDs, the Velocity-Azimuth Display (VAD) wind profile from the Boise WSR-88D, and estimated terrain induced boundary layer winds for the southwest corner of Idaho. The thermodynamic plot shown in Fig. 5 displays an inverted-V sounding (somewhat similar to a hybrid sounding). Lifting a surface parcel gives a CAPE of $930 \text{ m}^2 \text{ s}^{-2}$; only marginal instability when compared to the areas east of the Rockies. From subjective experience so far in Boise, this value appears to be marginal to moderate for this area. The actual instability at the time of storm initiation could be quite different since the thermodynamic profile was smoothed using gridded data at mandatory levels.

The hodograph (Fig. 6) was developed using assumed boundary layer winds below 2 km MSL, VAD winds from the Boise WSR-88D at 2022 UTC, and NGM forecast winds from PC-GRIDDs at 1800 UTC using the 1200 UTC model run. The boundary layer winds were generated using model-derived boundary layer flow and subjectively adjusting the direction and speed for terrain effects near the initiation region of the splitting storm. The VAD/NGM winds above the boundary layer were in excellent agreement. The accuracy of the subjectively estimated boundary layer winds is much more uncertain. Additionally, the terrain in the area of thunderstorm initiation is higher than at Boise, so the first few points of the hodograph were positioned on top of the 1.5 km value.

The modified hodograph depicts a shear of 23 m s^{-1} (length of the hodograph) from 1.5 to 6 km. The shape is basically unidirectional (straight hodograph), especially above the boundary layer, though some counterclockwise curvature is noted. Comparing this hodograph to the conceptual hodograph in Fig. 7 (from Fig. 15.16b in Weisman and Klemp 1986, but rotated 90° counterclockwise) and considering the significant vertical shear in Fig. 6, a splitting updraft would be favored. The "left-mover" (to be referred to as LM) would propagate to the north at a slower speed than the east-northeastward propagating "right-mover" (RM). With the slight counterclockwise curvature found in this case, the LM storm should be more dominant with an expected anticyclonic updraft rotation. The RM storm should be weaker and have a cyclonically rotating updraft.

More evidence of the expected dominance of the LM storm can be seen in the storm-relative (SR) inflow in Fig. 6 (dashed lines for LM storm and dashed-dot lines for RM storm). Calculations show a SR mean inflow (1.5 to 3 km layer) of 20 m s^{-1} from 320° for the LM storm which is marginally supportive of supercell development. Though less impressive, the SR mean inflow of 16 m s^{-1} from 20° for the RM storm is still significant, but less than 20 m s^{-1} .

WSR-88D Examination

An attempt to depict the evolution of the splitting storm using 0.5° reflectivity data from the WSR-88D at Boise is illustrated in Figs. 8a-c (obviously, the best way to view this evolution is with time-lapse display). At 1802 UTC (Fig. 8a), a single northeastward moving thunderstorm cell can be seen on the southwestern Idaho-northern Nevada-southeast Oregon border. By 1826 UTC (Fig. 8b), the cell splits into two distinct reflectivity maximums, neither one of which looks particularly impressive. One hour later at 1924 UTC (Fig. 8c), the tracks of the two storms reveal the distinct deviant motion compared to the initial path of the parent cell in Fig. 8a. The direction of motion of the LM storm was from 200° at 14 knots while the RM storm tracked from 244° at 24 knots. Initial parent storm motion (Fig. 8a) was from 225° at 16 knots (which should be a suitable estimate of the ambient mean wind in the cloud-bearing layer). Thus, the motion and speed of these two storms is in excellent agreement with the conceptual hodograph in Fig. 7. The LM storm was slower and slightly more dominant, per the more deviant motion, than the faster RM storm.

Fig. 8d exhibits the storm-relative velocity display at the 1.5° elevation angle at 1826 UTC. Radial shear can be calculated by the simple formula:

$$\frac{(V_I + V_O)}{2}$$

where V_I is the inbound radial velocity and V_O is the outbound radial velocity. Close examination reveals cyclonic radial shear of approximately 20 m s^{-1} on the right flank of the reflectivity maximum of the RM storm (compare with Fig. 8b). Much weaker anticyclonic radial shear ($\sim 14 \text{ m s}^{-1}$) is evident on the left flank of the LM storm. Radial divergence is also evident, centered on the reflectivity maximum of the LM storm. Once again, this arrangement agrees quite well with the numerical model depiction of a left-moving anticyclonic updraft and a right-moving cyclonic updraft under moderate to strong unidirectional vertical wind shear (Fig. 1a,b), though the magnitude of the radial shear is not as strong.

At 1924 UTC, the WSR-88D indicated a mesocyclone on the right flank of the LM storm (Fig. 9a). This cyclonic shear pattern was on the right side of a strong zone of radially outbound winds (northerly component) centered on the reflectivity maximum of the LM storm. The mesocyclone algorithm flagged this cyclonic circulation on the right flank of the storm, while a strong, undetected anticyclonic rotation persisted on the left flank of near-equal intensity ('x' in Fig. 9a). This corresponds to the east and west side of the radially outbound velocities (orange), respectively. Note that the WSR-88D mesocyclone algorithm does NOT search for anticyclonic circulations, even if the radial shear meets the specified criteria. In the conceptual framework (Fig. 1b), the pattern described above would correspond to the anticyclonic updraft (left flank circulation) and the cyclonic downdraft (right flank circulation) of the LM storm.

Interestingly, this storm had remarkably similar features to those found in a recent study by Houze et al. (1993) of damaging hailstorms in central Switzerland. They found several instances of left-moving storms with a "false hook" (Fig. 10b). Model simulations of the Swiss storms showed this cyclonic vortex ('c' in Fig. 10b) to be associated with downdraft air. This vortex in the Swiss storm is in a position similar to the right flank mesocyclone in the Idaho LM case (Fig. 9a). There is even a slight hint of the false hook in the reflectivity pattern of the Idaho LM storm, indicated by the pixel of 50 dBZ on the southeast edge (Fig. 9b). Anticyclonic shear was found on the northwest (inflow) side of the Swiss storms, near a region of strong reflectivity gradient, which is also similar to the strong gradient on the northwest side of the Idaho LM storm (cf. Figs. 9b and 10b). This dominant right flank cyclonic shear/false hook structure is in contrast to the mirror-image left-moving supercell (Fig. 10a).

After 1924 UTC, the LM storm began to dissipate. The RM storm merged with the slower moving cells to the northeast (seen in Fig. 8c) and formed a small line with a very short bowed-out segment. Near the time of merger, one inch diameter hail was reported near Grasmere, Idaho, which verified a severe thunderstorm warning that was issued earlier for the splitting storm system. No other verification was possible due to the sparse population in southwest Idaho.

Summary and Conclusions

The splitting storm system on 27 May 1994 agreed well with numerical model simulations of storms initiating in unidirectional vertical shear. The CAPE and vertical shear were marginal for supercellular development and splitting storms. Neither cell displayed strong evidence of supercellular characteristics such as an inflow notch, an obvious weak echo region, or strong and persistent rotation. Identification of inflow into each of the storms was difficult to determine due to the distance of the storms from the radar (center of the beam was at 15 Kft ASL at 0.5° slice). Alternatively, the storms were well-organized, lasting for 1.5-2.0 hours. Both storms also exhibited weaker rotational signals which were qualitatively similar to patterns expected by numerical simulations. Several other storms in the area were much more pulse-like and weaker (in terms of reflectivity), dissipating within thirty minutes to one hour. The LM storm was more quasi-steady, but both the LM and RM storms went through pulsing periods appearing similar to organized multi-cell storms at times. In summary, it would be quite difficult to categorize these storms.

Several important points are brought to light by this study:

- Boundary-layer winds are difficult to determine in complex terrain and this creates difficulties in determining the low-level vertical wind shear on the hodograph.
- Conceptual model features do appear in the West and can be captured by the WSR-88D, though complicated variations are likely to be common. Being familiar with these conceptual models can help to focus the meteorologist's attention on the more important storms and can help him/her to understand the structure and evolution of the radar-observed storms.
- Terrain features could have easily influenced the initiation and evolution of the splitting storm along with other mesoscale forcing not resolvable on current operational models. Thus, it cannot be said for certain that the evolution of this splitting storm can be completely explained by the mechanisms suggested in the three-dimensional model simulations.
- 0-3 km SR-helicity was difficult to assess due to the uncertain low-level shear profile in the vicinity of the storms. It seems more appropriate to concentrate on sfc-6 km shear and the shape of the hodograph in complex terrain.

References

- Houze, R.A., Jr., W. Schmid, R.G. Fovell, and H.H. Schiesser, 1993: Hailstorms in Switzerland: Left movers, right movers, and false hooks. *Mon. Wea. Rev.*, **121**, 3345-3370.
- Klemp, J.B., 1987: Dynamics of tornadic thunderstorms. *Ann. Rev. Fluid Mech.*, **19**, 369-402.
- Klemp, J.B. and R.B. Wilhelmson, 1978a: The simulation of three-dimensional convective storm dynamics. *J. Atmos. Sci.*, **35**, 1070-1096.
- ___, and ___, 1978b: Simulations of right- and left-moving storms produced through storm splitting. *J. Atmos. Sci.*, **35**, 1097-1110.
- Weisman, M.L. and J.B. Klemp, 1982: The dependence of numerically simulated convective storms on vertical wind shear and buoyancy. *Mon. Wea. Rev.*, **110**, 504-520.
- ___, and ___, 1984: The structure and classification of numerically simulated convective storms in directionally varying wind shears. *Mon. Wea. Rev.*, **112**, 2479-2498.
- ___, and ___, 1986: Characteristics of isolated convective storms. *Chapter 15, Mesoscale Meteorology and Forecasting*, P.S. Ray, editor, *Amer. Meteor. Soc.*, Boston, MA, 331-358.
- Lemon, L.R., and C.A. Doswell III, 1979: Severe thunderstorm evolution and mesocyclone structure as related to tornadogenesis. *Mon. Wea. Rev.*, **107**, 1184-1197.
- Moore, J.T. and G.E. VanKnowe, 1992: The effect of jet-streak curvature on kinematic fields. *Mon. Wea. Rev.*, **120**, 2429-2441.
- Wilhelmson, R.B., and J.B. Klemp, 1978: A numerical study of storm splitting that leads to long-lived storms. *J. Atmos. Sci.*, **35**, 1974-1986.

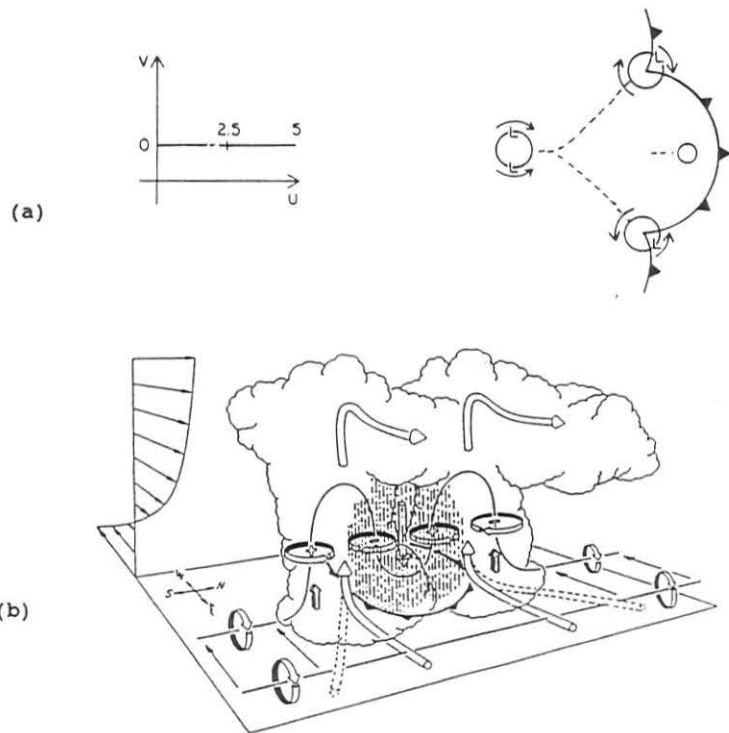


Figure 1. Schematics of storm splitting. (a) Updraft evolution in moderate to strong wind shear for unidirectional wind shear profile. Hodograph on left shows unidirectional shear to 5 Km. Circles on right depict updrafts with paths shown by dotted lines. Early stage is shown by single updraft on left with mid-level mesolow pressure on each flank (L). Mature phase on right exhibits two mesolows with the left/right moving storms turning anticyclonically/cyclonically. Barbed lines are surface gust fronts. (b) shows splitting of updraft as downdraft bends vortex tubes. Circular arrows depict the two pairs of cyclonic (+) and anticyclonic (-) mid-level circulations. The "left-mover" is shown on the right side of the schematic (anticyclonic on outside flank in region of updraft). (For further details see Klemp, 1987).

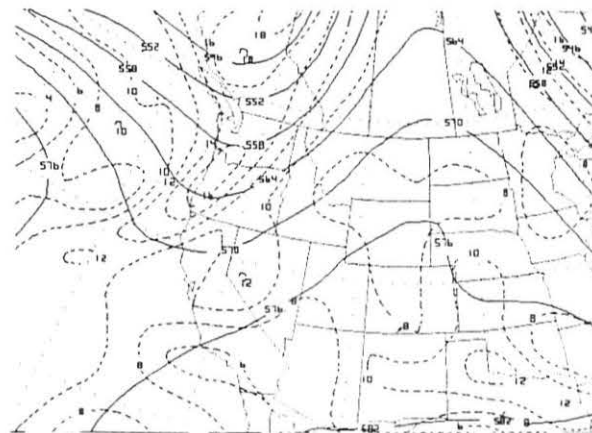


Figure 2. NGM 06 hour forecast of 500 mb geopotential height (solid) and absolute vorticity (dashed) valid at 1800 UTC 27 May 1994. Heights in dam at 60 m intervals. Vorticity at $2 \times 10^{-5} \text{ s}^{-1}$.

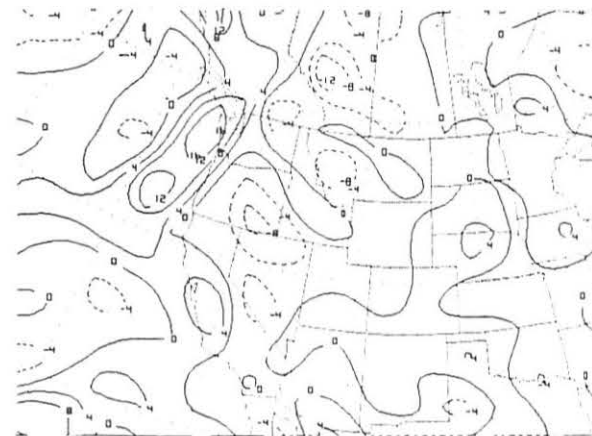


Figure 3. NGM 06 hour forecast of layer-averaged Q-vector divergence valid at 1800 UTC 27 May 1994. Divergence of Q is solid and convergence of Q is dashed. Layer-average is centered at 500 mb and extends from 700 to 400 mb. Contours at $4 \times 10^{-15} \text{ mb}^{-1} \text{ s}^{-3}$. (Static stability is not involved in calculation.)

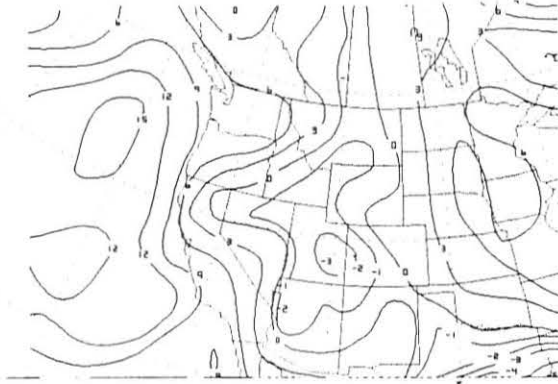


Figure 4. NGM 06 hour forecasted lifted indices valid at 1800 UTC 27 May 1994. Values less than zero contoured every 3°.

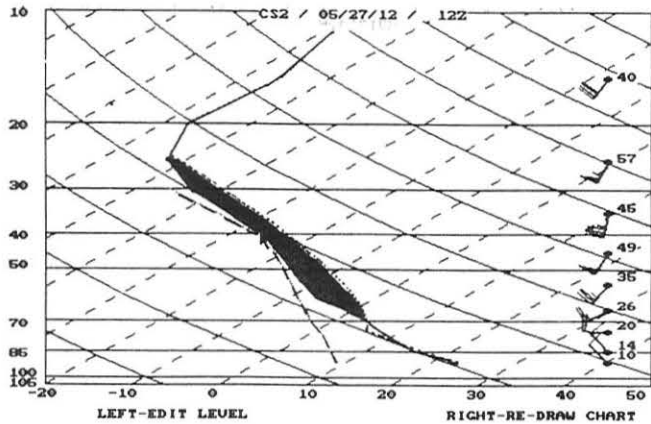


Figure 5. Thermodynamic profile for southwest corner of Idaho at 1800 UTC 27 May 1994. Shaded is positive area proportional to upward parcel motion. Approximate latitude/longitude for this modified sounding is 42.0/117.0.

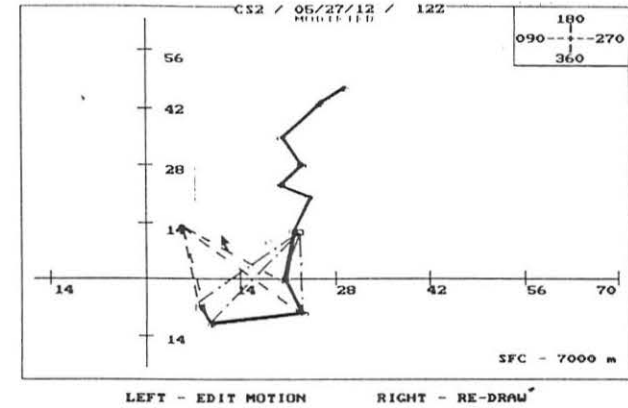


Figure 6. Hodograph at 1800 UTC 27 May 1994 for southwest corner of Idaho. Speeds are in knots. Vertical intervals (marked by open circles) are 0.5 Km apart starting at 1.5 Km. Dashed and dashed-dotted lines depict storm-relative inflow for the LM and RM storms, respectively. Filled circle (square) at apex of dashed (dashed-dotted) lines represents storm motion of LM (RM).

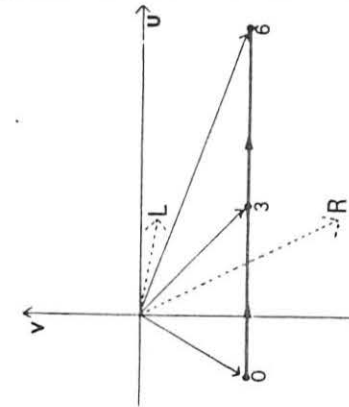
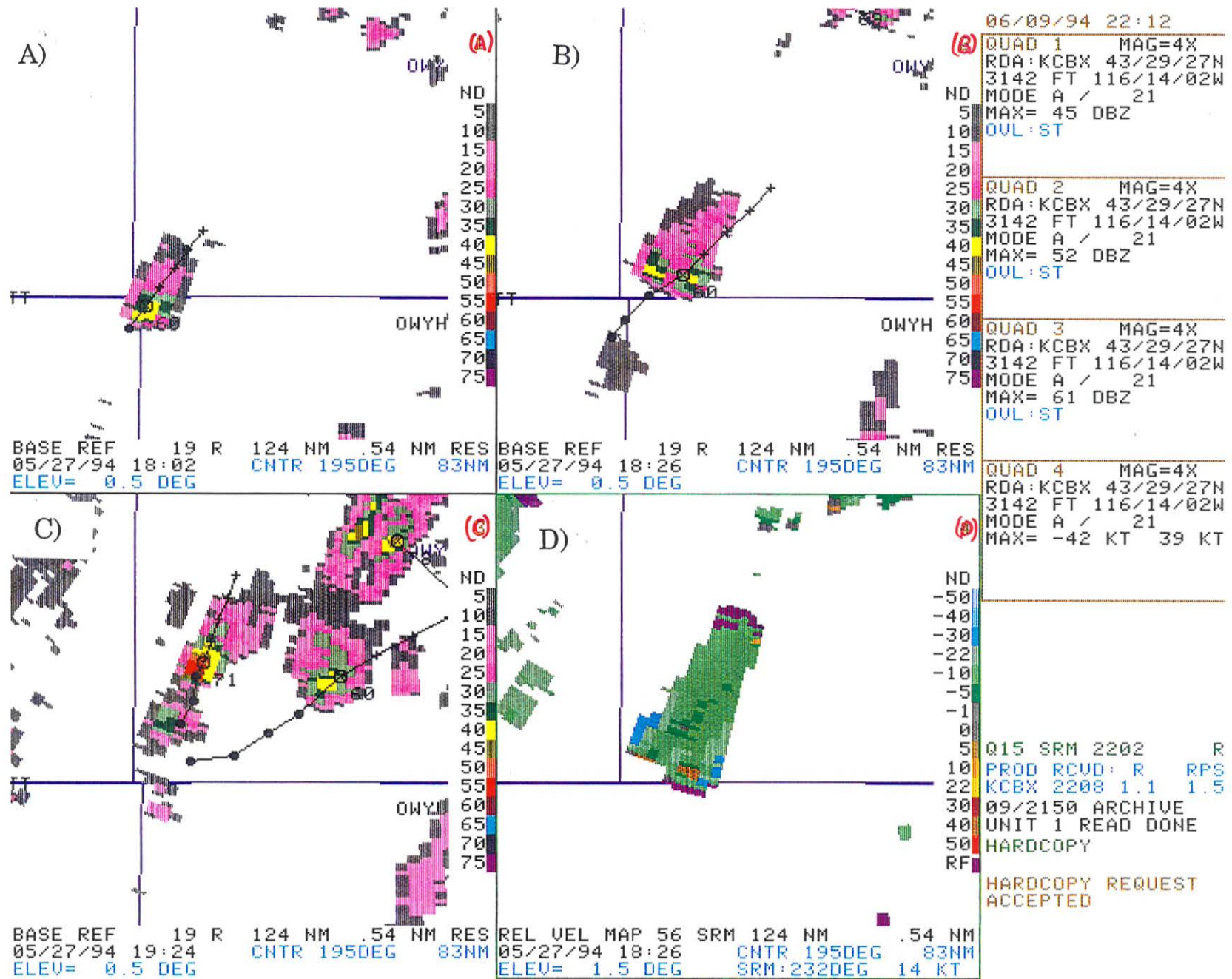


Figure 7. Conceptual hodograph with motion of split storms (L and R for left/right movers) relative to unidirectional vertical wind shear. Heights in Km. Thin solid vectors depict ground-relative winds. Thin dashed vectors show ground-relative storm motions. Thick vectors are the hodograph. (from Weisman and Klemp, 1986). Hodograph has been rotated by 90° counterclockwise to have a similar orientation with figure 6.

Figure 8.



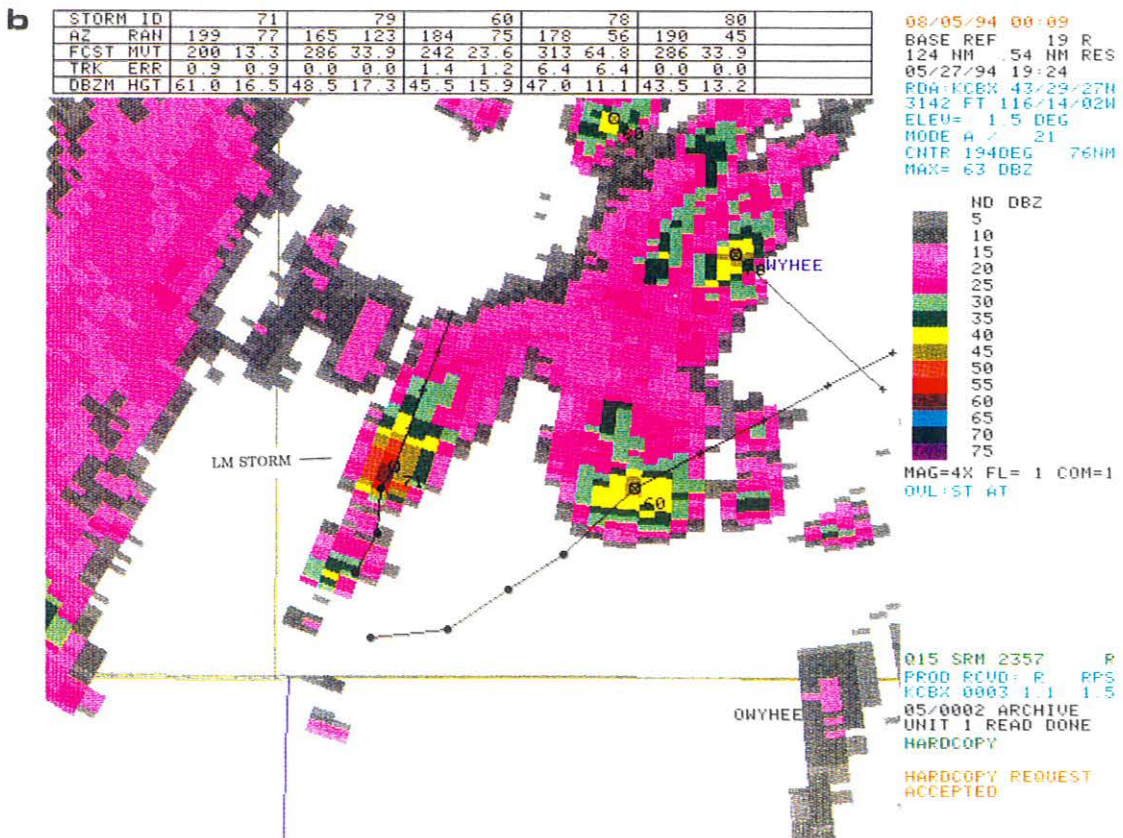
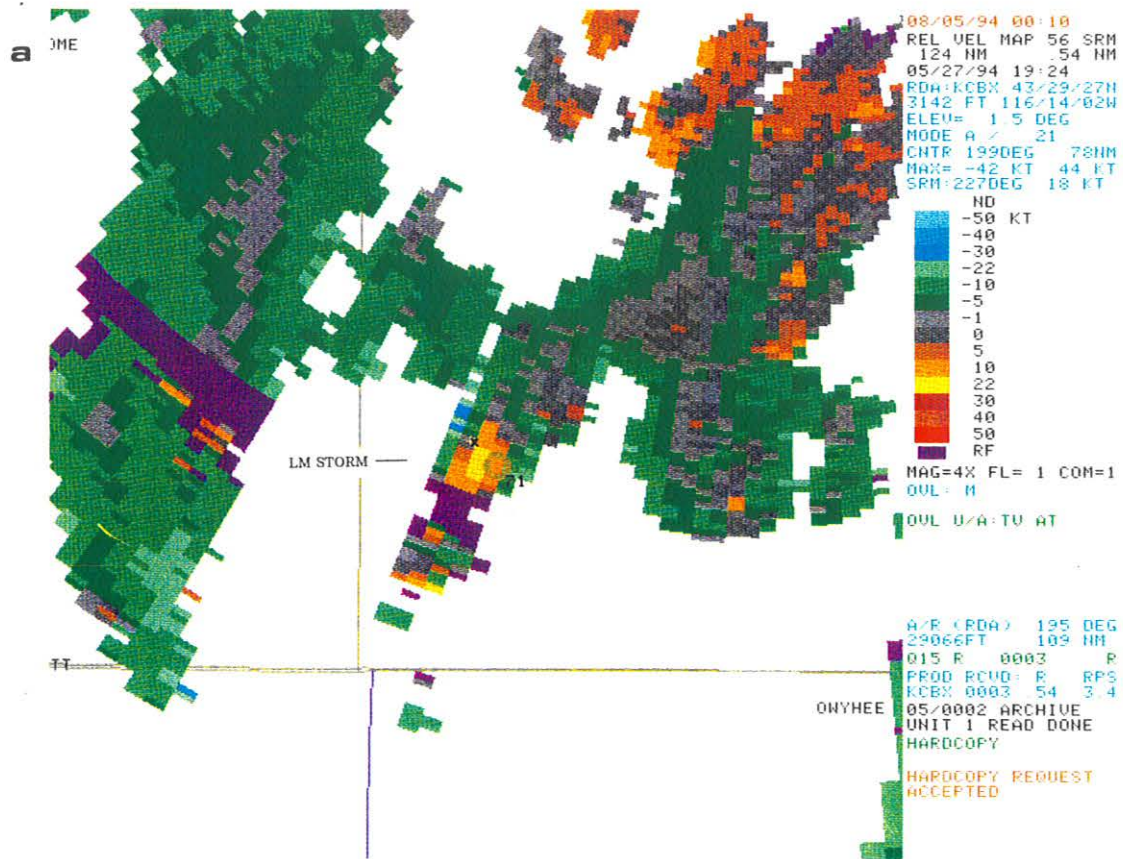


Figure 9. (a) WSR-88D relative velocity map product from KCBX (Boise, ID) at 1924 UTC 27 May 1994. Elevation angle 1.5°, ring indicates mesocyclone detection within cyclonic shear on right flank of the LM storm. (b) same as (a), except base reflectivity with storm tracking algorithm overlaid.

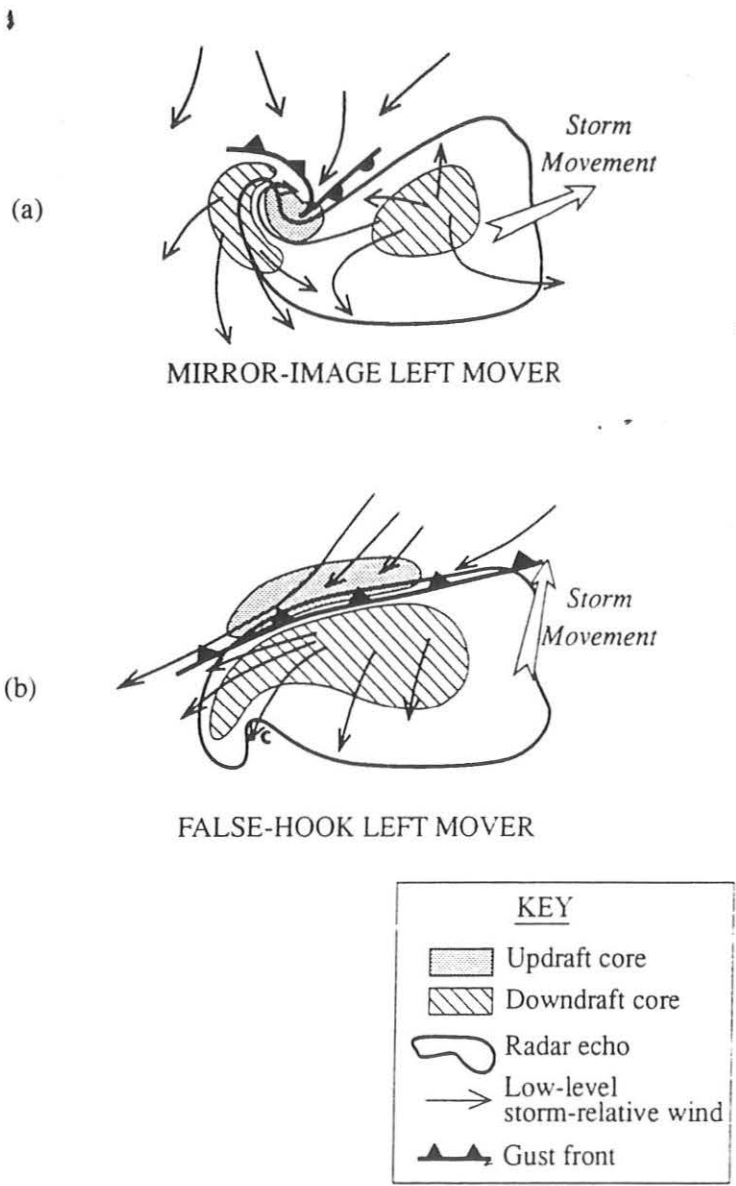


Figure 10. Idealized low-level kinematic and radar reflectivity structure of (a) a mirror-image of a classic supercell [adapted from Lemon and Doswell (1979)], and (b) a false hook left-mover as seen in the Swiss cases.